MONTHLY WEATHER REVIEW

VOLUME 94, NUMBER 2

FEBRUARY 1966

TESTS OF THE DIAGNOSTIC-CYCLE ROUTINE IN THE INTERPRETATION OF LAYER-CLOUD EVOLUTIONS[1]

ROLAND E. NAGLE, JAMES R. CLARK, AND MANFRED M. HOLL

Meteorology International Incorporated, Monterey, Calif.

ABSTRACT

A Routine is described which is a collection of computer-programed techniques designed for the interpretation of meteorological satellite videograph observations. From the inferred evolution of the mass-structure distribution, the Routine diagnoses the horizontal velocity distribution for one or more isentropic surfaces. Using the horizontal velocity distribution as input, the Routine further derives net horizontal and net vertical, parcel-displacements (in the synoptic range of scale) for specified regions and periods of time. This permits pattern configurations of layer-cloudiness to be remapped to later positions which are consistent with the mass-motion evolutions.

The use of the Routine for interpreting satellite cloud observations is illustrated by the presentation of two case studies. The layer-cloudiness distributions for the initial and terminal times of each case are analyzed primarily from the TIROS operational nephanalysis. The initial distribution of layer-cloudiness is remapped in accordance with the net horizontal displacement field. The cloud evolutions are shown and comparisons are made between the joint 24-hr. cloud displacement and net vertical, parcel-displacement patterns and the verifying layer-cloudiness distributions.

A close correspondence is found between the terminal position of the displaced cloudiness and the verifying cloudiness distributions. The patterns evolved in the horizontally displaced cloudiness are realistic reflections of the stages of development associated with vortex cloud patterns. Net vertical, parcel-displacement fields are generated which are consistent with conventional synoptic desiderata and the observed cloudiness. The results indicate that the major portion of layer-cloudiness distributions in the synoptic range of scale in extratropical latitudes can be accounted for by the time-integrated, horizontal and vertical parcel-displacements. The implications of these results to the objective use of satellite data are discussed.

1. INTRODUCTION

The TIROS series of satellites have amply demonstrated that instrumented, artificial earth satellites are highly efficient vehicles for observing the atmosphere. The videographs of the earth's cloud cover reveal equally clearly the distribution and pattern of cloudiness over regions of both good and poor conventional data coverage. In the interim since the successful launching of the first TIROS, a great amount of effort has been expended in attempting to relate cloud patterns to desiderata of middle-latitude synoptic meteorology. The results of these studies, which were recently consolidated in a comprehensive report by Widger [14], have been expressed in the useful but highly descriptive vernacular of the synoptician.

While the primary efforts of meteorological satellite research have been focused on the traditional air mass and frontal model approach to weather analysis and forecasting, the quantitative, numerical approach has not been completely overlooked. The recent literature contains several examples of studies devoted to determining relationships between various cloud patterns and atmospheric mass-motion fields. Hansen and Thompson [6] investigated the relationship between vertical motions computed by several methods and satellite cloud observations. Oliver [13] studied relationships between vorticity maxima and clouds, while Brodrick [2] concentrated on

[1] The studies reported here were sponsored by the Meteorological Satellite Laboratory of the National Weather Satellite Center, U.S. Weather Bureau under Contract No. Cwb-10884.

vorticity advection. Brooks and Shenk [3] systematically correlated cloud patterns with thermal and wind parameters. Although more than a casual relationship has been found between these parameters and various features of cloudiness, it can be stated that the results obtained in these investigations are not sufficiently precise to allow their routine categorical use.

For the past three years, the authors have been working toward the development of objective techniques for exploiting meteorological satellite observations. Our efforts have led to the development and testing of a system which has been given the appellation "The Diagnostic-Cycle Routine".

The Diagnostic-Cycle Routine is an assembly of computer-programed techniques designed for the interpretation of meteorological satellite cloud observations. The relevancy of the Routine to the objective exploitation of meteorological satellite observations is based on the premise that layer-cloudiness is related to the preceding evolution of the air parcels rather than to the current distribution of mass and/or motion parameters. The Routine is designed to process from the inferred evolution of the mass-structure,[2] the evolution of the concurrent motion fields with ageostrophic detail. From the mass-motion evolution, the Routine exhibits for specified periods of time and for a selected isentropic surface (or surfaces) the horizontal and vertical time-integrated parcel-displacements. This allows pattern configurations of layer-cloudiness to be rationally interpreted in terms of the mass-motion evolution.

The formulation of the Diagnostic-Cycle Routine was documented by Holl [8]. A preliminary test of the Routine using a combination of objective and time-consuming, subjective procedures was reported on by Holl, Clark, and Nagle [10]. This paper describes the Routine and presents results of its use in several case studies.

2. COMPONENT SUBROUTINES OF THE DIAGNOSTIC-CYCLE ROUTINE

The subroutines which constitute the Diagnostic-Cycle Routine and their sequence of operation are shown schematically in figure 1. In this section, the functions of these subroutines are briefly described. For a full documentation of the formulation the interested reader is referred to the original reports cited in the subsections below.

BASIC MASS-STRUCTURE ANALYSES

Within the operations of the U.S. Fleet Numerical Weather Facility (FNWF), there is available the 12-hourly analysis of the mass structure of the atmosphere in terms of a seven-parameter model. This model, developed by Holl, Bibbo, and Clark [9], is defined in terms of five layers, in each of which a specially defined static stability parameter is independent of the pressure as vertical coordinate. The required mass-structure data are routinely processed in the following sequential operations: at radiosonde data points, the heights of the mandatory levels are transformed to yield a reference height, mean temperature, and a multi-layered stability structure. These latter parameters (enhanced by near past data) are analyzed objectively in the horizontal plane; by operating on these fields with linear transforms, it is possible to diagnose a height and temperature for any pressure level within the vertical limits of the model specification.

In the structure model, the principal dependent parameters consist of: the 1000-mb. height, the 1000–500-mb. thickness, and the five static stability distributions. These data are stored on master data tapes for each map time; all fields are expressed in terms of a standard 63 x 63 grid-point array referred to a polar stereographic projection of grid length 381 km. at 60° N. Secondary dependent parameters of the mass-structure are also stored on the master data tapes; these include the height and temperature fields for the mandatory pressure levels from 1000 to 200 mb. The surface pressure field for a Berkofsky and Bertoni [1] smoothed topography is also available on the master data tapes.

Definition of the mass-structure in terms of the structure model utilized by the FNWF permits the extraction of well-defined isentropic analyses for any potential temperature surface within the vertical limits of the atmosphere encompassed by the model. The fields contained on the FNWF master data tapes constitute the basic input data for the Diagnostic-Cycle Routine.

PROGRAM ONE

Program One extracts the required mass-structure data from the FNWF master data tapes. For each selected map time, 11 parameters of the mass-structure are called in from the master data tape; Program One diagnoses for specified isentropic surfaces the pressure field, p_θ, and the Montgomery stream function field, Ψ_θ. The program also diagnoses the distribution of the pressure thickness,

$$\delta p_\theta = p_{\theta+2.5K} - p_{\theta-2.5K} \tag{1}$$

which enters into a mass continuity parameter, S, defined by:

$$S \equiv -\partial p/\partial\theta \tag{2}$$

This parameter is used in Program Three to modify the diagnosed wind in accordance with the inferred field of momentum convergence for the layer. The 12-hourly isentropic analyses and the concurrent terrain pressure are stored on magnetic tape for later processing. These activities are accomplished on the CDC–1604 computer; running times amount to about 1 min. 10 sec. for each isentropic level and for each synoptic map time.

[2] By virtue of the hydrostatic equation and the gas law, the three-dimensional distribution of air density also prescribes the distribution of pressure, virtual temperature, virtual potential temperature, corresponding lapse rates, etc. All these distributions are jointly referred to as the "mass" structure of the atmosphere.

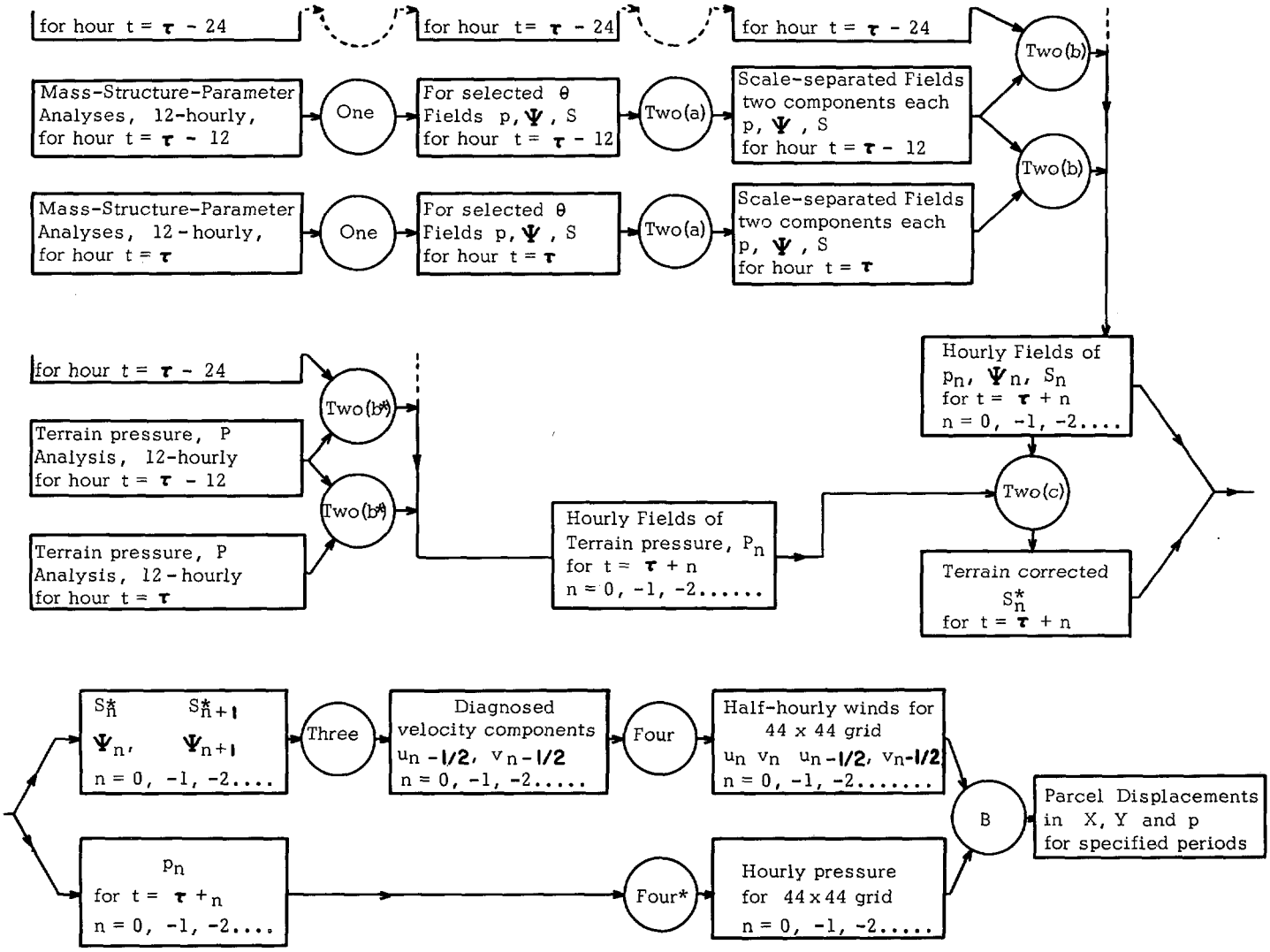

FIGURE 1.—Sequence of operations in application of the Diagnostic-Cycle Routine.

PROGRAM TWO (a)

This program is identified as the scale separation program. It is based on a technique, developed by Holl [7], which objectively and quantitatively separates a scalar field into recognizable and characteristic features embodied in the distribution. The technique utilizes an operator that functions in a manner which is analogous to the diffusion of heat in a two-dimensional plane. The original field is progressively "smoothed" by repeated application of the operator until the amplitude of a specified scale of component is reduced to less than 10 percent of its initial value. The operator is linear and therefore all additions and subtractions to yield subcomponents of the field are commutative. As used in the Diagnostic-Cycle Routine, the fields of p_θ, Ψ_θ, and δp_θ are separated into their disturbance and residual components (these components are analogous to the migratory pressure systems and the long-wave patterns respectively). Program Two (a) can be run on either the CDC–1604 or the CDC–3200 computers; running time for each 12-hr. diagnostic period is about 5 min.

PROGRAM TWO (b) AND TWO (b*)

Program Two (b) interpolates in time the 12-hourly distributions of p_θ, Ψ_θ, and δp_θ to yield hourly distributions of these parameters. This is accomplished in the following manner:[3] the residual components of p_θ, Ψ_θ, and δp_θ are linearly interpolated to hourly values. The hourly interpolated fields of the residual component of Ψ_θ serve as an evolving frame-of-reference steering field, from which the *disturbance* components of p_θ, Ψ_θ, and δp_θ are interpolated to hourly values. Total hourly fields of these requisite parameters are then produced by recombining fields of the disturbance components with the respective interpolated fields of the residual components.

[3] For an analytical discussion of this program see Holl [7].

Program Two (b*) interpolates the terrain pressure to hourly values by a local frame interpolation. Both of these programs are run on the CDC–1604 computer; running time is about 5 min. per field for each 12-hr. diagnostic period.

PROGRAM TWO (c)

The diagnosis of the pressure-height of one or both of the isentropic surfaces bounding δp_θ (see equation (1)) may involve a fictitious downward extension of the atmosphere's mass-structure to levels beneath the terrain; the correct measure of the pressure thickness of the air in this layer requires the removal of the portion below the terrain.

Program Two (c) processes the hourly distributions of the mass continuity parameter, S, to adjust for the below the ground portion of the δp_θ fields. The program utilizes the hourly interpolated values of terrain pressure. The terrain-corrected pressure thickness, S^*, replaces S according to

$$S^*=\begin{cases} S & \text{when } p_g \geq p_\theta + S/2 \\ p_g-(p_\theta-S/2) & \text{when } p_\theta+S/2>p_g>p_\theta-S/2 \\ 0 & \text{when } p_\theta-S/2 \geq p_g \end{cases} \tag{3}$$

where p_θ represents the pressure of the selected isentropic surface and p_g represents the terrain pressure.

The CDC–1604 computer is used for this program; *running time is about 1 min. for each 12-hr. diagnostic* period.

PROGRAM THREE

Program Three diagnoses a horizontal velocity distribution $\mathbf{V}_H$, from the distributions of the mass continuity parameter, S^*, the Montgomery stream function, Ψ_θ, and the mass-structure tendency, $\partial S^*/\partial t$. The diagnosed wind is based on the geostrophic approximation modified to accommodate the inferred field of momentum convergence for the layer. That is,

$$\mathbf{V}_H=\mathbf{V}_g+(1/S^*)\nabla\chi \tag{4}$$

$$\mathbf{V}_g=\mathbf{k}\times f^{-1}\nabla\Psi \tag{5}$$

$$\nabla^2\chi=-\partial S^*/\partial t-\nabla\cdot S^*\mathbf{V}_g \tag{6}$$

where $\mathbf{V}_g$ represents the geostrophic wind and χ is the momentum potential function. This diagnosed velocity satisfies the quasi-adiabatic, mass-continuity equation,

$$\partial S^*/\partial t=-\nabla\cdot(S^*\mathbf{V}_H) \tag{7}$$

This program, run on the CDC–1604 computer, requires about 10 min. for each 12-hr. diagnostic period.

PROGRAM FOUR AND FOUR*

Program Four extracts, from the output of Program Three, the hourly winds for a selected 22 x 22 subregion of the basic 63 x 63 grid-point array. It generates half-hourly winds for the 22 x 22 subregion by interpolating between the hourly values and, in addition, interpolates this field spatially to produce an expanded 44 x 44 array based on the original 22 x 22 subregion. Program Four* extracts the hourly pressure of the selected isentropic surface. On the CDC–1604 computer, these operations require about 1 min.

PROGRAM B

Using the output of Program Four, Program B first evolves the x, y, parcel-displacement fields in accruing periods of 6, 12, 18, and 24 hr. From the terminal position of the parcels for the intervals and the pressure distributions at the initial and terminal times, the net change in pressure of each parcel along its trajectory can be readily determined. The final output of the Diagnostic-Cycle Routine are line-drawn distributions of the x, y, and p parcel-displacement fields. These permit an initial distribution of layer-cloudiness to be manually remapped to later positions and also allow the net isentropic ascent and descent of the parcels to be examined. The running time for this program is about 3 min. on the CDC–1604 computer.

3. SELECTION OF CASES AND CLOUD ANALYSIS PROCEDURES

Cases for analysis were selected on the basis of several criteria; prerequisite were: a subregion possessing a reasonable information density in the mass-structure analysis, sufficient satellite videograph coverage over this subregion to allow an adequate depiction of the layer-cloudiness distribution, and an interesting synoptic development. The population of potential cases for analysis included TIROS VII and VIII observations during the period January 1, 1964 through January 1, 1965. Five cases were analyzed in the original study (see Nagle, Clark, and Holl [11]); two of these are presented in this paper.

The delineation of the layer-cloudiness presented certain problems. As the Diagnostic-Cycle Routine was formulated to treat layer-cloudiness associated with synoptic-scale processes, convective cloudiness and cloudiness generated by sub-synoptic-scale processes (i.e., orographic clouds, diurnal cumulus, etc.) should therefore be excluded from the analysis. It is difficult, however, to specifically identify cloud forms in the TIROS videographs; (see for example, Erickson and Hubert [5] and Conover [4]). As a consequence, the delineation of regions of layer-cloudiness involved considerable subjective interpretation. When the daily TIROS nephanalyses were surveyed it became apparent that the symbolic legends used in the nephanalyses provided a rational basis for differentiating synoptically significant areas of layer-cloudiness. Layer-cloudiness was defined

by the following symbolic classification used in the operational nephanalyses: clouds within areas enclosed by "scalloped" borders (boundaries of major cloud systems) and identified by (1) stipling (". . . areas considered by the analyst to be of greatest synoptic significance") and (2) areas of 80 percent or greater coverage. In addition, mostly covered areas, MCO, (50–80 percent coverage) were included when it was apparent that they were integral components of organized cloud systems.

Because of the "off-time" nature of the satellite observations, it was necessary to blend the successive swaths into a composite nephanalysis corresponding to the time of upper-air observations. This was accomplished in the following manner: the TIROS swath closest to the time of the upper-air observations was used as the base for the layer-cloudiness nephanalysis. Preceding and successive swaths were then adjusted to the cloudiness portrayed in the base swath. When these "off-time" swaths fell over a land area with a dense observations network, the surface cloud observations were used to assist in the adjustment of the satellite-observed patterns. In certain cases, "off-time" satellite swaths over oceanic areas did not overlap swaths coincident with the upper-air observations; no attempt was made to adjust the position of the cloudiness depicted in these swaths. In addition, the coverage by satellite observations was never complete over the entire analysis subregions; therefore, over the continental United States surface observations were used to supplement the TIROS nephanalyses. All nephanalyses were constructed independently of the numerical portion of the experiments. Without exception, the layer-cloudiness distributions were prepared prior to, and were not modified after, the receipt of the output of the Diagnostic-Cycle Routine.

The procedure for arriving at the horizontal displacement of the layer-cloudiness is illustrated in figure 2. The initial parcel-labeling field is shown in figure 2a superimposed upon the corresponding layer-cloudiness distribution. Several points on the layer-cloudiness boundary have been identified with alphabetical symbols to facilitate their later recognition. The parcel-labeling field, displaced in accordance with the net 18-hr. horizontal trajectories, is shown in figure 2b. The initial cloudiness of figure 2a was then remapped to its later position; this was accomplished by manually drawing the cloud boundaries on the displaced parcel-labeling field according to the cloud boundaries position in respect to the labeling lines. For example, points A and C of figure 2a are located near x, y intersections (26,26) and (23,23) respectively; these two points were relocated on the displaced parcel-labeling field of figure 2b. The line segment connecting these two points was then drawn with attention being paid to maintaining the initial cloud-to-no-cloud proportionality in each x, y module.

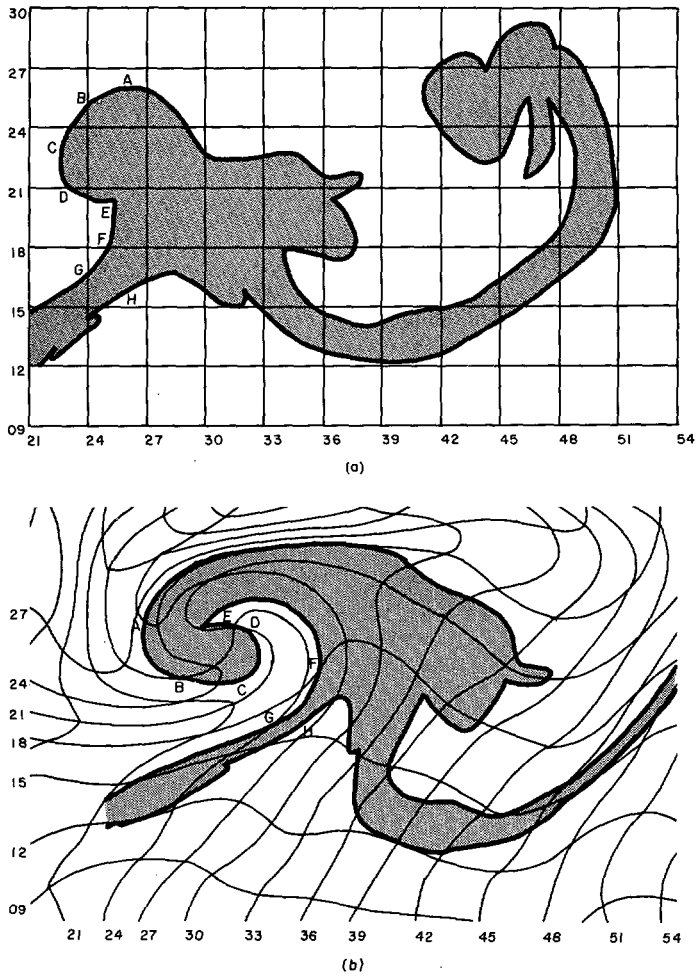

FIGURE 2.—Example of the procedure used for remapping the initial cloudiness distribution in accordance with the horizontal displacement field.

4. CASE STUDIES

Two cases are now presented to illustrate the capabilities of the Routine. In the first, the evolution of the cloudiness at cumulative 6-hr. intervals covering a 24-hr. period are presented. In the second case, the cloudiness evolution is omitted and only the 24-hr. displacement pattern is shown. In this latter case, analyses were performed at two different isentropic levels.

CASE I: 1200 GMT, FEBRUARY 15, TO 1200 GMT, FEBRUARY 16, 1964

Our primary interest in this case was focused on a rapidly deepening low pressure system which developed over the Texas Panhandle early on February 15, 1964. The surface synoptic charts for 1200 GMT, February 15, and February 16, are shown in figures 3 and 4, respectively. By 1200 GMT, February 15, the developing low pressure system was located over northeastern Oklahoma with a minimum pressure of 1000 mb. During the suc-

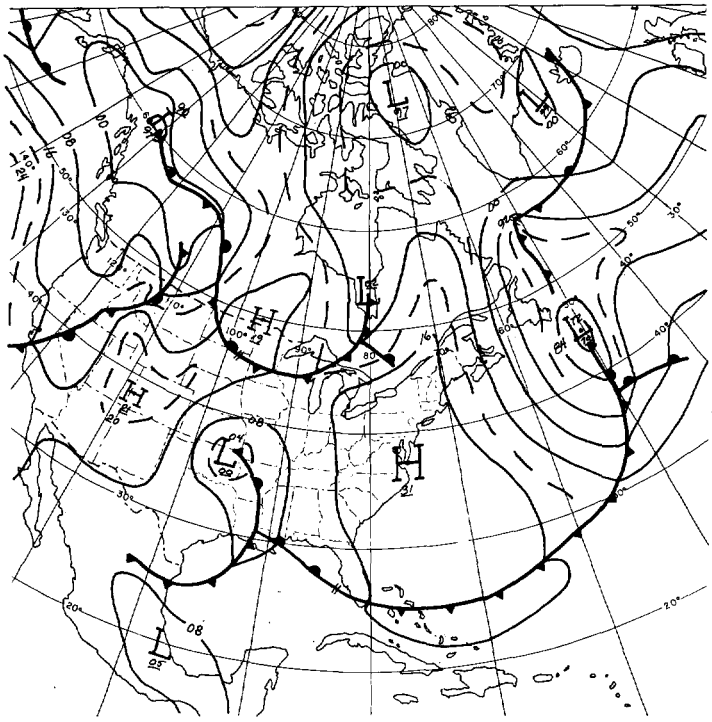

FIGURE 3.—Surface analysis, 1200 GMT, February 15, 1964.

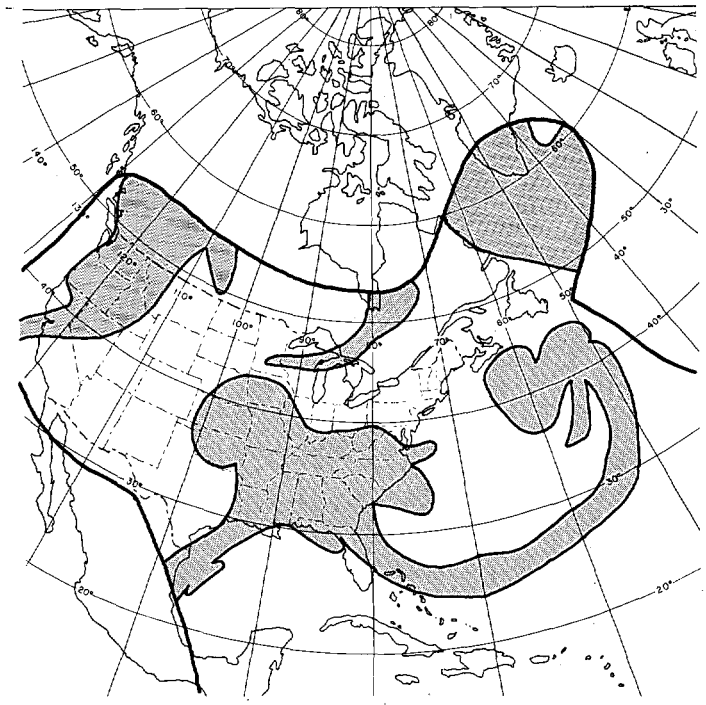

FIGURE 5.—Initial layer-cloudiness analysis, 1200 GMT, February 15, 1964.

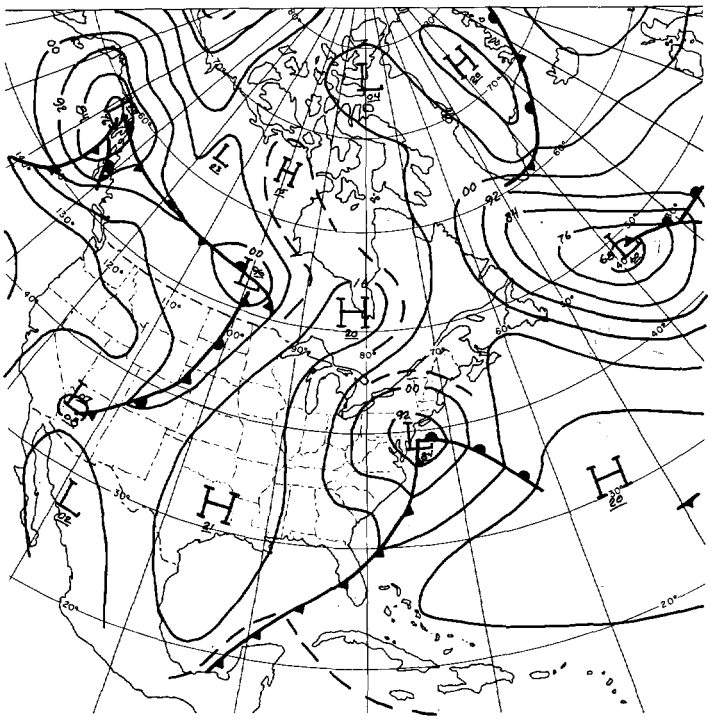

FIGURE 4.—Surface analysis, 1200 GMT, February 16, 1964.

ceeding 12-hr. period, this center moved steadily northeastward and by 0000 GMT, February 16, was located over southern Indiana with a central pressure of 996 mb. At this time a secondary low pressure system developed at the apex of the occlusion over central Georgia; this latter system showed marked development and moved rapidly up the east coast of the United States. By 1200 GMT, February 16, the Georgia Low had become the dominant system and was located off the Delaware coast with a central pressure of 984 mb. The surface frontal system during this period moved rapidly through the southeastern United States and by 1200 GMT, February 16, paralleled the east coast over the western Atlantic. Aloft, a deep trough in the westerlies attended these surface developments. The 305° K. potential temperature isentropic surface was chosen for the analysis.

In figure 5 is shown the layer-cloudiness analysis for 1200 GMT, February 15. This nephanalysis is based on satellite data obtained from TIROS VII orbital passes 3564, 65, 66, 67 and TIROS VIII pass 816. Characteristic features observed in satellite videographs are evident in this layer-cloudiness pattern which can be readily related to the classical frontal model cloud distribution. An elongated frontal band extended from a low-pressure center south of Newfoundland to the Florida-Georgia coast. Extensive pre-warm-frontal cloudiness covered the central Atlantic and Southeastern States; and a "comma"-shaped cloud pattern associated with the developing low pressure system was located over the Central Plains States.

The layer-cloudiness evolution at 6-hr. intervals, superimposed on the cumulative, net vertical, parcel-displacement fields, is shown in figure 6. It is instructive to consider first only the displaced layer-cloudiness patterns. In this manner, the chronological development of the intruding clear tongue so characteristic of major cloud-

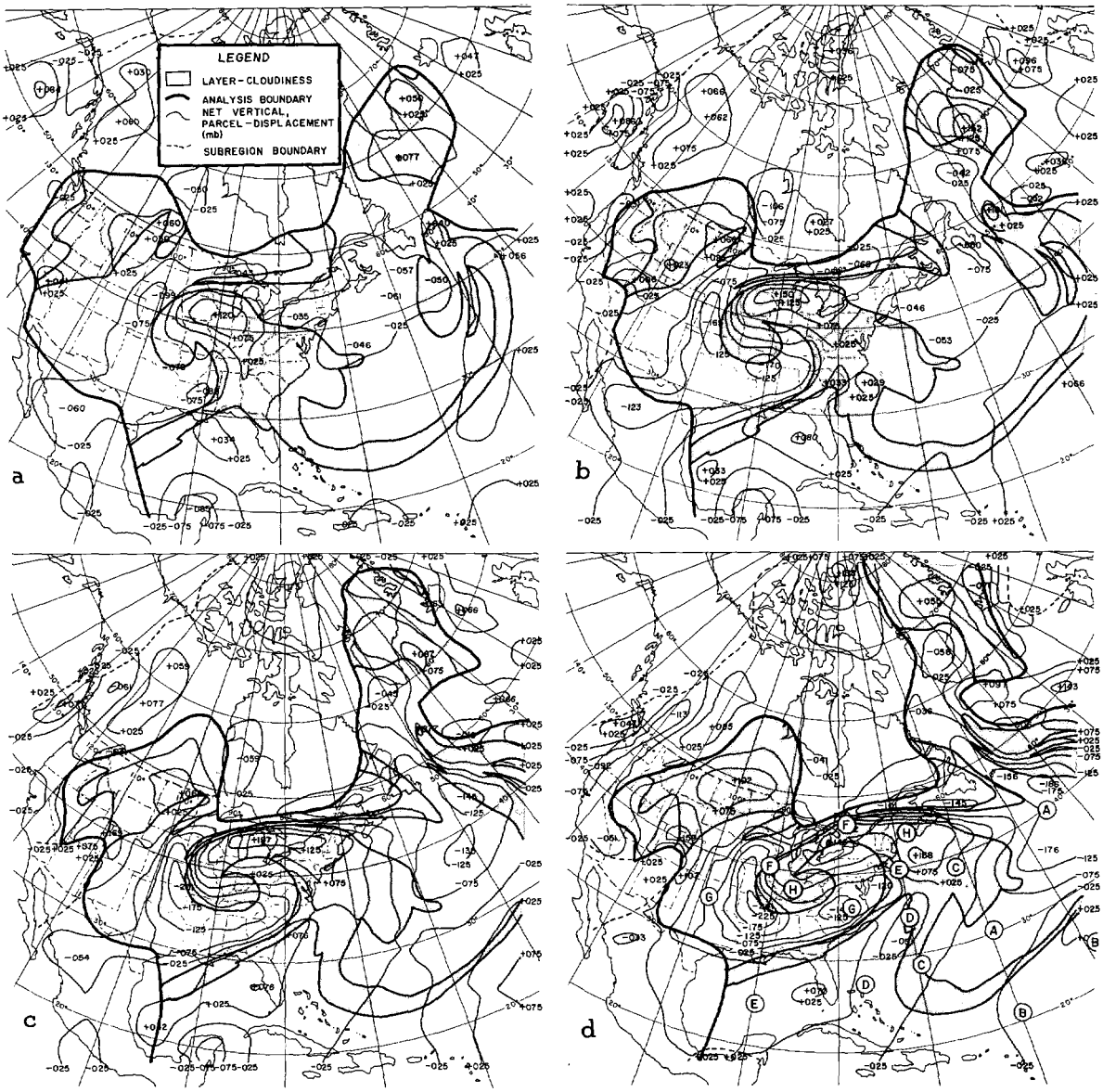

FIGURE 6.—Layer-cloudiness evolution and the attendant vertical parcel-displacement, 1200 GMT, February 15 to 1200 GMT, February 16, 1964 (a) 6-hr.; (b) 12-hr.; (c) 18-hr.; (d) 24-hr.

vortex patterns, can be readily followed. The clear tongue observed on the initial layer-cloudiness distribution over central Texas (see fig. 5), intruded rapidly to the north and east into previously cloud-covered geographical regions. The differential motion of the cloud-free[4] and cloud-covered areas evolved into a spiral configuration within the 24-hr. analysis period. Relative parcel rotation during this period amounted to about 180 deg. along the northwestern periphery of the "comma"-shaped cloud mass. This pattern of evolution corresponds almost identically with Widger's [14] model depicted in his figures 4 through 8.

[4] As used in this paper, "cloud-free" denotes an absence of layer-cloudiness, i. e., not necessarily a clear area.

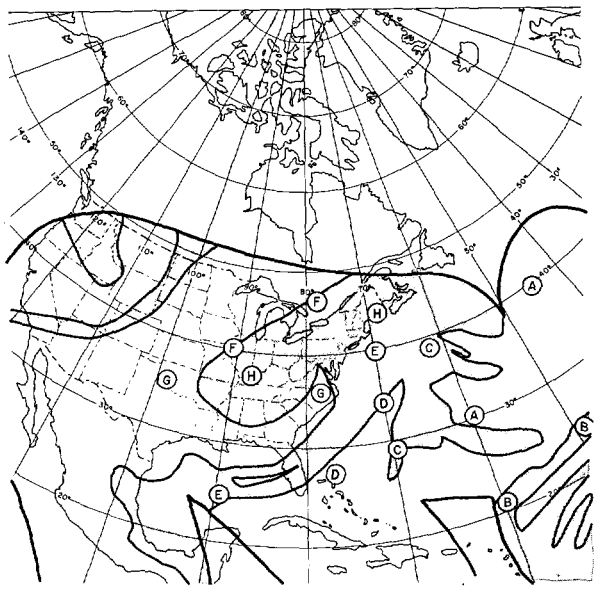

FIGURE 7.—Verifying layer-cloudiness analysis, 1200 GMT, February 16, 1964.

Figure 7 shows the verifying layer-cloudiness distribution corresponding to the 24-hr. displacement of figure 6d. Specific features have been labeled on figures 6d and 7 to facilitate the comparison. In the discussion below, features of the verifying layer-cloudiness analysis are compared jointly with the 24-hr. cloud and net vertical, parcel-displacements.

A—A *A large cloud-free area located southeast of Newfoundland.* This was associated with a cold air mass which had moved over the Atlantic from the North American continent. This cloud-free area corresponded in location and configuration to an area of net parcel descent.

B—B *An extensive cloud band.* This cloud band was associated with a dissipating cold front and was in close proximity to the terminal position of the frontal band which, on the initial layer-cloudiness distribution, extended from the low pressure system south of Newfoundland. This feature was also coincident with an area of weak, net parcel ascent.

C—C *An ill-defined cloud band.* This feature was apparently associated with the warm front which existed off the central Atlantic States. This cloud mass coincided with the terminal position of the western extreme of the above mentioned frontal band; it was an area of weak, net parcel ascent (less than 25 mb.). Although satellite videograph coverage was not complete, the section of the frontal band between B—B and C—C apparently dissipated through the action of subsidence.

D—D *An extensive cloud-free tongue.* This area was located in the warm sector of the western Atlantic frontal system. This feature coincided with both an intruding cloud-free tongue and a net parcel descent maxima (minus 51 mb.).

E—E *A prominent and extensive band of cloudiness.* This feature was associated with the cold front which was parallel to the east coast of the United States. North of Cape Hatteras the displaced cloudiness pattern coincided with the verifying cloud distribution. In the southerly extremes it closely corresponded to a region of net parcel ascent.

F—F *A major cloud boundary.* This cloud boundary corresponded with both the terminal position of the northern extent of the pre-frontal cloud shield and a col area between net parcel ascent and descent.

G—G *An extensive clear tongue.* This clear tongue was contained entirely within the cold air mass of the storm. It corresponded closely both to the location and configuration of the intruding post-frontal clear tongue and to the axis of an extensive area of net parcel descent. Two major centers of descent were present: one of minus 149 mb. located over North Carolina and a second of minus 241 mb. over Arkansas.

H—H *An extensive area of "up-slope" cloudiness.* This feature constituted the major cloud shield of the storm. It coincided almost exactly with the combined displaced cloudiness and areas of net parcel ascent.

An area where only fair agreement was evident was located over the Mississippi-Alabama region of the United States. In this area the actual cloudiness on the verifying analysis was more extensive than indicated by the net vertical, parcel-displacement pattern. The clouds viewed in the original videographs (not shown) over Mississippi and Alabama appeared to be of a cumuliform nature. The fact coupled with the existing synoptic conditions suggested that these clouds were stratocumulus and should not have been included in the verifying layer-cloudiness distribution.

CASE II: 1200 GMT, OCTOBER 18, TO 1200 GMT, OCTOBER 19, 1964

Case II was chosen almost at random to investigate the applicability of the Diagnostic-Cycle Routine to a typical situation. Extensive videograph coverage was available over considerable portions of the North American continent on the two consecutive days of the analysis period. A prominent cloud feature was also evident in the videographs. Analyses were performed on both the 305° K. and the 315° K. potential temperature surfaces; comparisons are made between the 24-hr. displaced cloudiness patterns at these two levels and variations from the verifying layer-cloudiness distribution.

The surface synoptic charts for 1200 GMT October 18, and October 19, 1964, are shown in figures 8 and 9, respectively. Of particular concern was the occluded frontal system which extended from the low pressure area located over Hudson Bay at 1200 GMT, October 18. During the analysis period, the center of this system moved east-southeastward with little change in pressure and was located over northern Quebec by 1200 GMT, October 19. During this period, the occluding portion of the frontal system moved eastward through the Province of Quebec while the cold front trailed through the central and eastern United States. Aloft, an intense long-wave trough dominated the entire eastern portion of the North American continent. This pattern changed very little during the 24-hr. period.

The layer-cloudiness analysis for 1200 GMT, October 18, is shown in figure 10. This analysis was based on TIROS VIII orbital passes 4379, 81, 82, and 83. The cloud band associated with the occluding frontal system was clearly evident. The 24-hr. horizontally displaced cloudiness pattern superimposed on the corresponding net vertical, parcel-displacements for the 305° K. potential temperature surface is shown in figure 11. Significant features have again been identified to facilitate the comparison with the verifying layer-cloudiness analysis which is shown in figure 12.

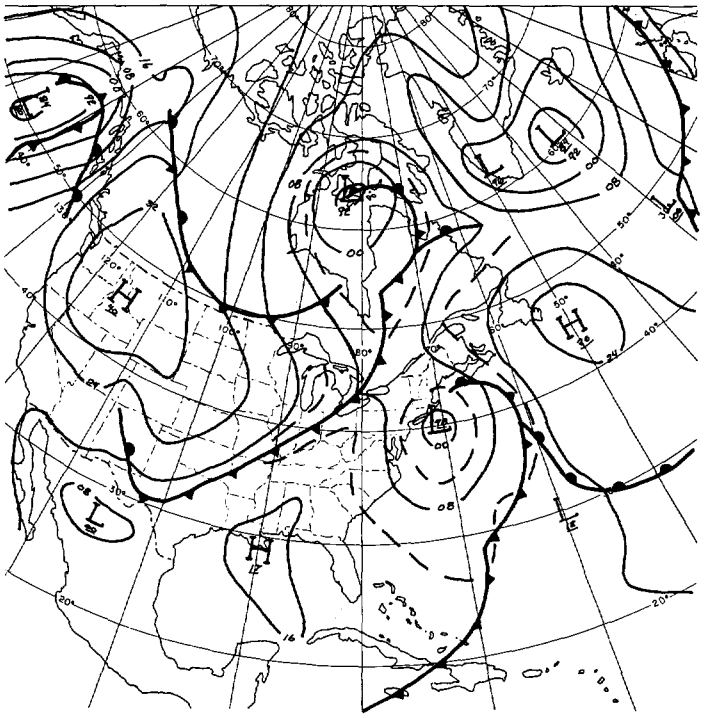

FIGURE 8.—Surface analysis, 1200 GMT, October 18, 1964.

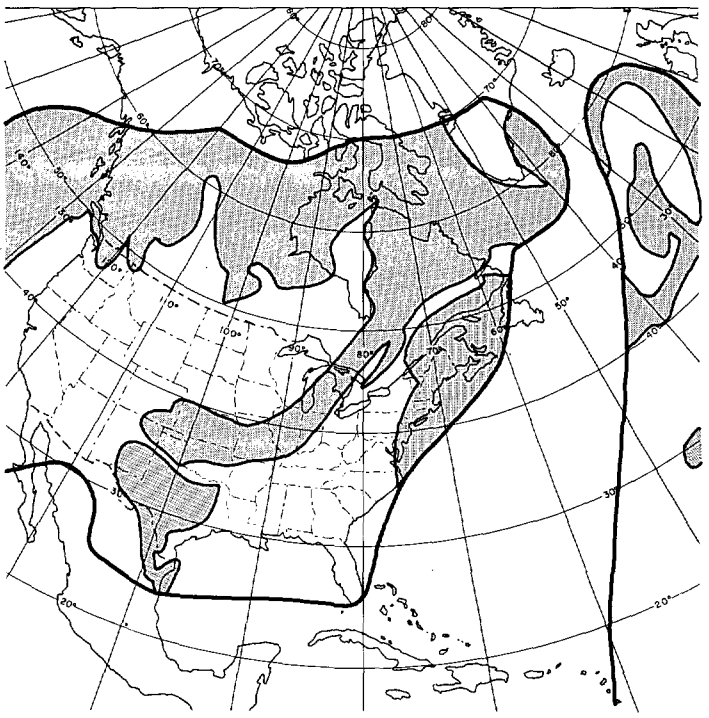

FIGURE 10.—Initial layer-cloudiness analysis, 1200 GMT, October 18, 1964.

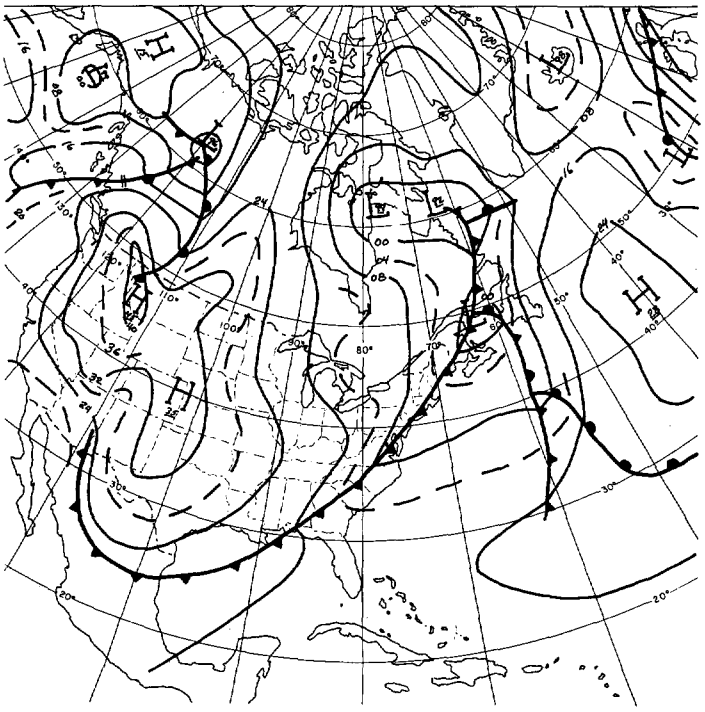

FIGURE 9.—Surface analysis, 1200 GMT, October 19, 1964.

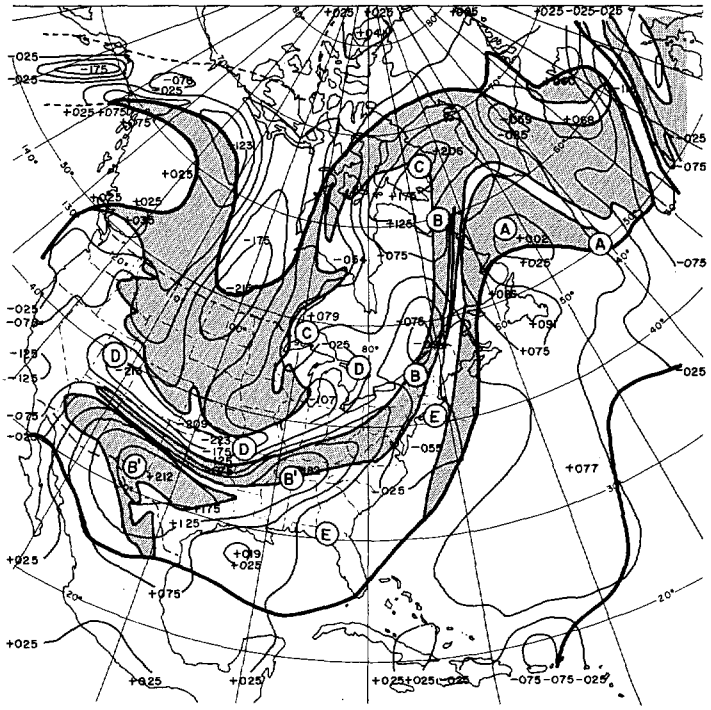

FIGURE 11.—The 24-hour displaced layer-cloudiness and the attendant vertical parcel-displacement, 1200 GMT, October 19, 1964 (305° K.). (For legend see fig. 6.)

A—A *A band of cloudiness which extended southeastward from the major prefrontal cloud shield of the storm system.* This feature was coincident with the terminal position of a layer-cloudiness area which had been associated with a dissipating low pressure system on the initial analysis. It also was a region of weak net parcel ascent.

B—B *A major cloud band.* This feature was associated with the occluded front. It coincided with the terminal position of the cloudiness that was previously associated with this same frontal system.

798-374 O-66—2

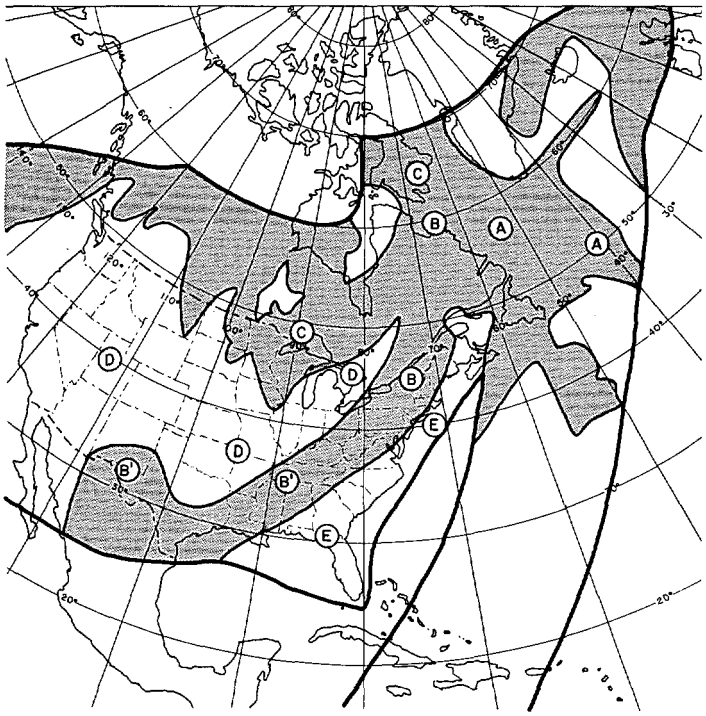

FIGURE 12.—Verifying layer-cloudiness analysis, 1200 GMT, October 19, 1964.

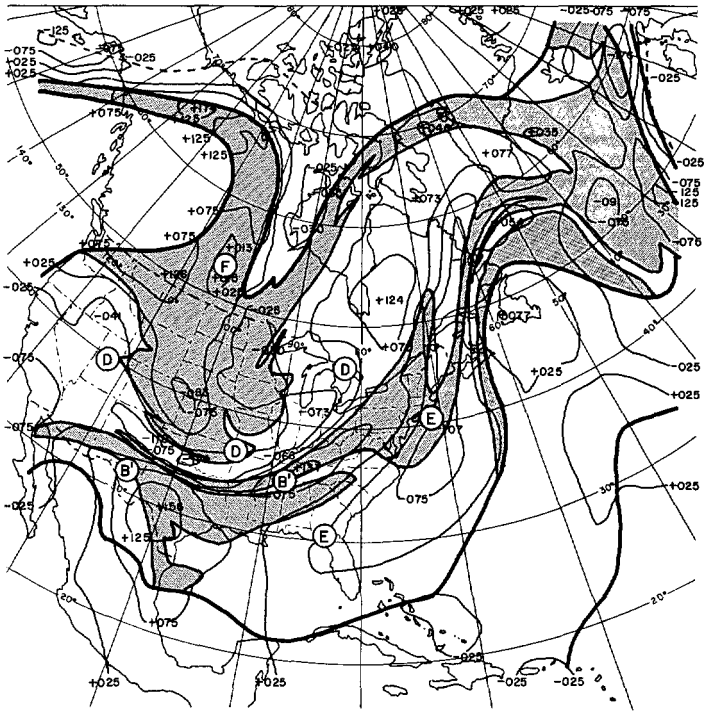

FIGURE 13.—The 24-hour displaced layer-cloudiness and the attendant vertical parcel-displacement, 1200 GMT, October 19, 1964 (315° K.). (For legend see fig. 6.)

B′—B′ *The southern portion of the above mentioned frontal band.* This feature coincided closely with the displaced cloudiness and, in addition, it was associated with an area of large-magnitude, net parcel ascents (maximum plus 212 mb.).

C—C *An extensive band of cloudiness.* This area of cloudiness was situated in the post-frontal region of the storm system. It was located within the area of the intruding cloud-free tongue; however it corresponded well in location and configuration with a region of net parcel ascent.

D—D *The post-frontal, cloud-free tongue.* This feature was intruding in the storm's cloud shield. It corresponded with portions of the displaced cloudiness distribution and also with an axis of large-magnitude, net parcel descent (maximum minus 223 mb.).

E—E *A pre-frontal, cloud-free tongue.* This area covered the southeastern Atlantic States and portions of the Canadian Maritime Provinces. It coincided exactly with a comparable cloud-free region in the displaced cloudiness distribution. South of Long Island, this system also corresponded to an area of net parcel descent.

The 24-hr. displaced layer-cloudiness pattern for the 315° K. potential temperature level, superimposed on the corresponding net vertical, parcel-displacement patterns for this surface is shown in figure 13. The cloudiness distribution shown in figure 10 was used as the initial analysis for this evolution; no attempt was made to distinguish the differential cloud heights in this analysis.

The pattern of the displaced cloudiness resembles that of the 305° K. potential temperature surface but reflects the stronger winds at the 315° K. isentropic surface. Several features are of particular interest. The intruding clear tongue on the 315° K. isentropic surface had advanced around the northern end of the high pressure ridge in the vicinity of Greenland during the 24-hr. period. The air parcels in the leading edge of this tongue underwent net lifting during the first 18 hr.; during the final 6 hr. of the analysis period the parcels were moving southeastward on the east side of the ridge line and were subsiding. This air originated in the post-frontal region of the system over eastern Canada and within 24 hr. was found some 500 mi. east of the surface frontal system; such a mechanism was suggested by Nagle and Serebreny [12] to account for an extensive clear area in the case study of cloudiness over the Gulf of Alaska.

The second feature of interest is the protruding cloud bulge which evolved within the intruding cloud-free tongue over New England and eastern Canada. This feature evolved from the western extreme of the frontal band which on the initial cloudiness analysis was located over eastern Colorado. There was no counterpart of this pattern on the 305° K. potential temperature surface. It

apparently reflected a region of strong horizontal shear on the upper isentropic surface which was not present in the motion field of the lower surface.

By comparing figures 11 and 13, a compatibility between the vertical displacement patterns at the 305° K. and 315° K. isentropic surfaces can be seen. In certain regions, the net vertical, parcel-displacement fields were similar at both levels. We refer to B′—B′, D—D, and E—E, where comparable features overlapped at both levels. This shows that identical features of the net vertical, parcel-displacement pattern existed through layers of up to 150-mb. thickness of these areas.

We also note area F on the 315° K. potential temperature surface. This marks an area of net parcel ascent which was displaced slightly to the west of a strongly descending area on the 305° K. potential temperature surface. The origin of these contrasting vertical displacement patterns is not clear; however it does indicate a necessity to consider more than one level of the atmosphere when interpreting the cloudiness distributions. A band of cloudiness, which corresponded in location and orientation to this area of ascent, existed in the verifying layer-cloudiness distribution (see fig. 12). This may have been high cloudiness but lack of cloud-height information deters further explanation.

5. DISCUSSION OF RESULTS

The results obtained in the application of the Diagnostic-Cycle Routine to interpret layer-cloudiness may be summarized as follows: (1) a close correspondence was found between the terminal position of the displaced cloudiness and the verifying cloudiness distributions; (2) patterns were evolved in the horizontally displaced cloudiness which are consistent with characteristic stages of development associated with vortex cloud patterns; and (3) the patterns of the net vertical, parcel-displacement fields were consistent with generally accepted vertical motion patterns associated with conventional synoptic desiderata, i.e., fronts, air masses, jet streams, etc., and the observed cloudiness.

While the results depended on the subjective comparison of the evolved and the verifying cloud distributions, they were, generally, mutually consistent. The preponderance of cloud-covered (cloud-free) regions in the verifying layer-cloudiness distributions corresponded with regions of ascent (descent) in the 24-hr. terminal position of the displaced cloudiness. In regions where the 24-hr. terminal position of the displaced cloudiness indicated a presence of cloudiness (absence of cloudiness) in contradiction to the verifying cloudiness distribution, the 24-hr. net vertical, parcel-displacement fields usually showed descents (ascents). The pattern of the net vertical, parcel-displacement fields showed a cellular structure whose elongated axes were aligned generally parallel to the direction of flow. This pattern usually became evident in the 12-hr. displacement field and became more pronounced at the 18- and 24-hr. intervals. With the more organized storm systems, the cellular structure consisted of alternating ascending and descending bands separated by large horizontal gradients; in addition, the pattern of the net vertical, parcel-displacement field was arranged in a spiral configuration.

The above suggests that the major portion of layer-cloudiness distribution can be accounted for by the time-integrated, horizontal and vertical parcel-displacements on a suitable isentropic surface (or surfaces). Two mechanisms are therefore of importance to the configuration of synoptic-scale, layer-cloudiness distributions as observed at a given instant of time: (1) generation (dissipation) of new cloudiness by lifting (subsidence) and (2) the quasi-horizontal advection and deformation of previously generated cloudiness. The distinction between convective and layer-cloudiness and the relative role of the above-mentioned mechanisms at various stages in the life cycle of extratropical cyclones is of great importance to a proper interpretation of the cloudiness patterns associated with such storms.

The implications of these results are of manifest importance to the objective use of meteorological satellite observations. The correspondence found in the cases investigated indicates that the hydrometeor-related significant variability of the atmosphere in the synoptic range of scale can be accounted for by quasi-geostrophic, adiabatic motion. Where lifting (subsidence) is accompanied by condensation (evaporation) with associated heating (cooling), the parcel ascent (descent) will be greater than that diagnosed under the adiabatic approximation. Therefore, it should be noted that the diagnosed vertical displacements are underestimates in regions where condensation or evaporation is occurring. It may be mentioned, in regard to the motion field, that the momentum-convergence component of the wind plays an essential role in forming the character of the vertical displacement patterns; this was determined by some comparative integrations using only the geostrophic wind. Layer-cloudiness distributions, therefore, contain direct information pertaining to isentropic displacements and, thereby, contain indirect, mass-structure information for corresponding isentropic surfaces. This suggests that the distribution of cloudiness at a particular instant of time will be highly correlated with concurrent mass-motion parameters (such as vertical motion) only when the instantaneous tendencies of these parameters coincide with the time-integrated effects. Thus, the objective use of information derived from satellite videographs in the existing constant-pressure-analysis system must include consideration of the prior history of the air parcels.

ACKNOWLEDGMENT

The accomplishment of the objectives of this investigation necessitated the extensive use of a medium capacity digital computer and auxiliary equipment. The U.S. Fleet Numerical Weather Facility contributed the use of computer facilities and peripheral

equipment for the performance of all numerical computations conducted in this investigation. Many of the charts reproduced in this report were drawn by the plot programs and automatic curve plotters of the FNWF. The contribution provided by the FNWF is gratefully acknowledged.

REFERENCES

1. L. Berkofsky and E. A. Bertoni, "Mean Topographic Charts for the Entire Earth," *Bulletin of the American Meteorological Society*, vol. 36, No. 7, Sept. 1955, pp. 350–354.
2. H. J. Brodrick, "TIROS Cloud Pattern Morphology of Some Mid Latitude Weather Systems," *Meteorological Satellite Laboratory Report* No. 24 (manuscript), U.S. Weather Bureau, Washington, D.C. Jan. 1964, 31 pp.
3. E. M. Brooks and W. E. Shenk, "Synoptic Studies of Vortex Cloud Patterns," *Final Report*, on Contract Cwb–10817, Geophysics Corporation of America, Bedford, Mass., Mar. 1965, 163 pp.
4. J. H. Conover, "Cloud Interpretation from Satellite Altitudes," *Research Note* No. 8. (suppl. 1), Geophysics Research Directorate, Air Force Cambridge Research Center, Cambridge, Mass., May 1963, 19 pp.
5. C. O. Erickson and L. F. Hubert, "Identification of Cloud Forms from TIROS I Pictures," *Meteorological Satellite Laboratory Report* No. 7 (manuscript) U.S. Weather Bureau, Washington, D.C. 1961, 68 pp.
6. J. Hansen and A. H. Thompson, "Vertical Motion Calculations and Satellite Cloud Observations over the Western and Central United States," *Journal of Applied Meteorology*, vol. 4, No. 1, Feb. 1965, pp. 18–30.
7. M. M. Holl, "A Diagnostic-Cycle Routine" *Final Report* on Contract No. 10314, Meteorology International Inc., Monterey Calif., Feb. 1963, 37 pp.
8. M. M. Holl, "Scale and Pattern Spectra and Decomposition," *Technical Memorandum* No. 3, on Contract N228–(62271)60550, Meteorology International Inc., Monterey, Calif., Nov. 1963, 28 pp.
9. M. M. Holl, J. P. Bibbo, and J. R. Clark, "Linear Transforms for State-Parameter Structure," *Technical Memorandum* No. 1, Edition Two, on Contract N228–(62271)58264, Meteorology International Inc., Monterey, Calif., Oct. 1963, 29 pp.
10. M. M. Holl, J. R. Clark, and R. E. Nagle, "A Test of the Diagnostic-Cycle Routine", *Final Report*, on Contract No. Cwb–10561, Meteorology International Inc., Monterey, Calif., May 1964, 83 pp.
11. R. E. Nagle, J. R. Clark, and M. M. Holl, "Evaluation of the Diagnostic-Cycle Routine in the Interpretation of Layer-Cloud Evolutions," *Final Report*, on Contract No. Cwb–10884, Meteorology International Inc., Monterey, Calif., May 1965, 87 pp.
12. R. E. Nagle and S. M. Serebreny, "Radar Precipitation Echo and Satellite Cloud Observations of a Maritime Cyclone," *Journal of Applied Meteorology*, vol. 1, No. 3, Sept. 1962, pp. 279–295.
13. V. J. Oliver, "Vorticity, Clouds and Weather," paper presented at the 225th National Meeting of the American Meteorological Society, Los Angeles, Calif., Jan. 1964.
14. W. K. Widger, Jr., "A Synthesis of Interpretations of Extratropical Vortex Patterns as Seen by TIROS," *Monthly Weather Review*, vol. 92, No. 6, June 1964, pp. 263–282.

[*Received August 27, 1965; revised November 8, 1965*]